Vol 15 No 7, July 2006
1009-1963/2006/15(07)/1602-09

Chinese Physics

© 2006 Chin. Phys. Soc.
and IOP Publishing Ltd

Monte carlo simulation of magnetization and coercivity of free magnetic clusters*

Huang Zhi-Gao(黄志高)†, Chen Zhi-Gao(陈志高), Jiang Li-Qin(蒋丽钦), Ye Qin-Ying(叶晴莹), and Wu Qing-Yun(吴青云)

Department of Physics, Fujian Normal University, Fuzhou 350007, *China*

(Received 29 December 2005; revised manuscript received 4 April 2006)

Based on Monte Carlo method, the oscillatory behaviour of the average magnetic moment as a function of the cluster sizes and the temperature dependences of magnetic moment with different sizes have been studied. It is found that the oscillations superimposed on the decreasing moment are associated with not only the geometrical structure effects but also the thermal fluctuation. The hystereses and thermal coercivities for free clusters with zero and finite uniaxial anisotropies have been calculated. The simulated thermal dependence of the coercivity is consistent with the experimental result, but does not fit the T^{α} law in the whole temperature range. It is evident that an easy magnetization direction and an anisotropy resulting from the spin configurations exist in the free clusters with the pure exchange interaction, which is also proved by the natural angle and energy distribution of clusters. A systematic theoretical analysis is also made to establish the relationship between natural angle and coercivity.

Keywords: Monte Carlo, cluster, magnetization, hysteresis
PACC: 7540M, 7560J, 7560E

1. Introduction

Two-dimensional (2D) magnetism has been extensively studied in ultrathin films and multilayers, leading to the discovery of several novel magnetic phenomena such as strong surface anisotropies, enhanced moments, and oscillatory interlayer exchange coupling.[1−4] The magnetic clusters in molecular beams (free ones), metals and semiconductors (ones embedded in the matrices) have become interesting topics in theory and experiment.[5] The spintronic materials with large tunnelling magnetoresistance (TMR) and giant magnetoresistance (GMR), such as granular films and tunnel-type nanostructures, have been found.[6−9] It is suggested that such a large magnetoresistance (MR) is due to the interplay of the relative orientation of magnetic moments between clusters, and the intrinsic characters of clusters in the spintronic materials.[10−13] Recently, the free clusters with no interaction between them and with no surrounding medium have also been studied.[14−16] It is significant for us to understand the magnetism because of the properties of an individual cluster rather than averaging over an ensemble. The magnitude of the magnetic moment per atom in the surface of free transition metal clusters can increase drastically with the distance from the surface due to band narrowing as a result of reduction in coordination number at the surface.[2,14−20] In those free clusters, there are two novel magnetic properties:[16] one is the average magnetic moment displaying an oscillatory behaviour as a function of the cluster size, and the other is the existence of special temperature dependence of magnetic moment. A few models have been established to explain the former result.[21−23] Based on the fact that the clusters are fabricated and magnetization is measured at a finite temperature,[14−16] the temperature effect should be taken into account. But, Jensen and Bennemann,[22] and Aguilera *et al*[23] did not consider the temperature effect in their model. Although Zhao *et al* took into account the temperature effect,[21] the simple Bloch $T^{3/2}$ law in the mean field approximation was only introduced. Up to now, the difference between theory and experiment does still remain and the explanation for the latter result is still an open question.

*Project supported by the State Key Program of Basic Research of China (Grant No 2005CB623605), the Natural Science Foundation of Fujian Province, China (Grant Nos E0320002 and 2005K020), the National Natural Science Foundation of China (Grant No 10474037).

†Corresponding author. E-mail: zghuang@fjnu.edu.cn

The classical mechanisms of hysteresis and coercivity for a non-interaction between randomly aligned single-domain particles with uniaxial anisotropy are known from the published classical papers by Stoner and Wohlfarth.[24] For an individual nanomagnet with strong size and surface effects, however, the theory presented by Stoner *et al* does not hold true. Recently, more and more nanomagnets, such as patterned magnetic nanostructures and clusters, have been used in spintronic and microelectronic devices. The hysteresis and anisotropy of the nanomagnets become interesting research subjects due to their strong surface and size effects. Recently, a new interesting idea called configurational anisotropy in the nanomagnets was suggested by Cowburn.[25] It comes from the differences between the energy configurations with the small deviations from the uniform magnetization. It has been considered in the elliptical, triangular, square, pentagonal and circular geometries.[25−28] However, up to now the configurational anisotropy of the free cluster has been hardly found. At the same time, another important concept called 'natural' angle was raised in study of exchange bias by Stamps *et al*.[29,30] The natural angle refers to the equilibrium orientation of the ferromagnet in a zero field applied. It is thought that the natural angle and configurational anisotropy could be significant to study the correlations among the hysteresis, anisotropy, natural angle and spin configuration in nanomagnet. In this paper, based on the Monte Carlo method, the oscillatory behaviour of the average magnetic moment as a function of the cluster size and the temperature dependence of magnetic moment with different sizes are studied. The hystereses and the thermal coercivities for the free clusters with zero anisotropy and for the block with periodic boundary (PB) conditions and finite uniaxial anisotropy are also studied. It is evident that an easy magnetization direction and an anisotropy resulting from the spin configurations exist in the free clusters with the pure exchange interaction. The natural angle and energy distribution of the clusters are calculated. The relationship between natural angle and coercivity are discussed, too.

2. Model and simulation method

It has been found that the magnitude of the magnetic moment per atom in the surface of free Fe, Co, Ni clusters can increase drastically with the decrease of coordination number in the surface.[2,14−20] Based on the Fridel's model [18] and a simplified rectangular d-band model,[21] the magnetic moment as a function of the local coordination number can be expressed as follows:

$$\mu_i = \begin{cases} (Z_{\rm b}/Z_i)^{1/2}\mu_{\rm b}, \text{if } Z_i \geq Z_{\rm b}(\mu_{\rm b}/\mu_{\rm dim})^2, \\ \mu_{\rm dim}, \quad \text{if } Z_i < Z_{\rm b}(\mu_{\rm b}/\mu_{\rm dim})^2, \end{cases} \tag{1}$$

where Z_i and $Z_{\rm b}$ are the coordination numbers of the ith atom in the surface and atom in the bulk, respectively; $\mu_{\rm b}$ and $\mu_{\rm dim}$ are the magnetic moments in the bulk and of dimmer, respectively. For Co atom, $\mu_{\rm b} = 1.72\ \mu_{\rm B}$ and $\mu_{\rm dim} = 2.33\ \mu_{\rm B}$. For simplicity, $\mu_{\rm B}$ is taken as the reduced unit of magnetization. The average magnetic moment per atom of the entire cluster can be described by

$$\boldsymbol{M} = \frac{1}{N}\sum_{i=1}^{N}\boldsymbol{\mu}_i(H,T), \tag{2}$$

where $|\boldsymbol{\mu}(H,T)| = \mu_i$, $M = |\boldsymbol{M}|$, H, T and N represent the applied magnetic field, the temperature and the total atom number of the cluster, respectively. At $T = 0$ K, the vector sum in Eq.(2) becomes a scalar sum because the magnetic moments of the atoms in the cluster are all in the ground states. At a finite temperature, however, the complex spin configurations resulting from the thermal excitation make Eq.(2) remain to be the vector sum. Compared with the previous studies,[[21−23] it is an important improvement to consider the temperature effect of spin configuration for Eq.(2).

The total spin Hamiltonian of the free cluster is described as follows:

$$H_{\rm s} = -\sum_{<ij>} J\boldsymbol{\mu}_i\cdot\boldsymbol{\mu}_j - K\sum_i(\mu_i^{\rm Z})^2 - H\sum_{i'}\mu_i^{\rm Z}, \tag{3}$$

where $\sum_{<ij>}$ is performed over the spin pairs at the nearest-neighbour (NN) sites i and j with exchange interaction J_{ij}, K is the uniaxial anisotropy with easy axis along the z-axis. In order to study the influence of spin configuration on the magnetic properties of the cluster, two types of clusters with FCC structure and the lattice constant a are considered. One is the free ferromagnetic cluster with K=0, which is referred to as a pure free ferromagnetic cluster (PFFC). The other is the free ferromagnetic cluster with uniaxial anisotropy ($K \neq 0$). In addition, in order to study the effect of shape on magnetization of the cluster, the atoms of the cluster are restricted to the ellipse shape described by $(i-i_0)^2 + (j-j_0)^2 + d(k-k_0)^2 = R_c^2$,

where (i_0, j_0, k_0) is for the origin, (i, j, k) for the lattice site in the ellipse surface, R_c for the radius of connecting circle between the ellipse and xy plane, d for the parameter controlling the shape of the ellipse. When $d = 1$, the ellipse becomes a sphere. When $d < 1$, it is an elongate shape. When $d > 1$, it is a flat shape. With different values of d, we can construct the clusters with variant shape. For example, when $d = 1$ and R_c=4.0, the number of atoms N in the cluster equals 249; when $d = 0.1$ and $R_c = 3.3$, $N = 247$; when $d = 2$ and $R_c = 5.5$, $N = 239$. For the spherical cluster with a radius R_c, it is assumed that the radius of the core is R_{core} and the thickness of surface shell remains constant ($R_c - R_{core} = a$), and only the particle size is varied. a is taken as the reduced unit ($a = 1$). The detailed structures are described in Ref.[31]. The cores and surface shells for the other ellipses can be defined in a similar way. The exchange interaction J_{ij} between the sites i and j in Eq.(2) is taken as J. J is used as the unit of temperature and also energy, and let $J = 0.5 \times 2.9$mRy.[20,32] Free boundary conditions are applied in all directions. In order to model the magnetic properties of the bulk materials, we use an $L \times L \times L$ block with periodic boundary (PB) conditions, FCC structure and the zero uniaxial anisotropy. In our simulation L is taken as 20.

The spin configurations of FCC magnetic clusters and block were simulated by standard Monte Carlo method (MC).[33] The principle of the algorithm has been introduced in our previous work.[[12,31,34,35]] Based on the experimental procedure, we started from a random configuration in a system studied that is at a high temperature and then cooled it quasicontinuously down to its measured temperature without or with a magnetic field applied. 400 Monte Carlo steps (MCSs) were performed at each temperature. The hysteresis loops were calculated in such a magnetic field that it started from a demagnetized state at $H = 0$ and increased quasicontinuously to H_m, then decreased to $-H_m$, and increased to $+H_m$, during which ΔH is taken as ~0.05 and the magnetization was averaged over ~2000 MCSs in each field. The simulation methods of the natural angle and the spatial distribution of energy under different directions of the applied magnetic field were described in our previous work.[36] The spherical polar coordinates θ and ϕ are divided into $N_n = (N_1 \times N_2)$ orientations (θ_l, ϕ_m), where $\theta_l = 0, \pi/N_1, 2\pi/N_1, 3\pi/N_1, \ldots, l\pi/N_1, \ldots, and \ \pi; \phi_m = 0, \pi/N_2, 2\pi/N_2, 3\pi/N_2, \ldots,$ and 2π. Each spin in the magnetic cluster always directs at orientation angle (θ_l, ϕ_m). As updating the spin orientation in visiting each atomic site, we can obtain the spatial distribution of spin orientation. If the equilibrium spin configuration of the magnetic cluster at zero applied field are obtained, the number of spins N_l orientating at θ_l can be obtained. Thus, the average natural angle can be computed by $\bar{\theta} = \sum_l \theta_l N_l / \sum_l N_l$.

3. Simulation results and discussion

The N-dependent average coordination numbers Z in the ground states for three typical shapes ($d = 0.1, 1.0$ and 2.0) and cuboctahedral structure are shown in Fig.1. One notes that the N-dependent Z for cuboctahedral structure [21] is almost the same as that for spherical FCC structure.

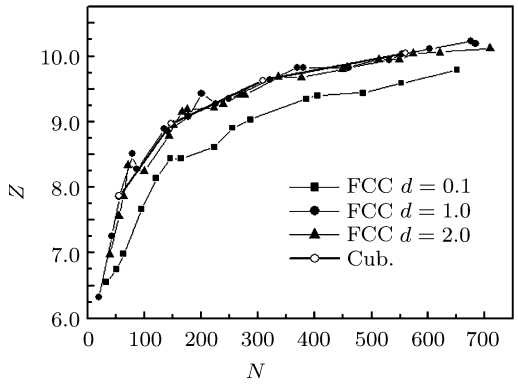


Fig.1. The N dependence of the average coordination number Z in the ground states for three typical shapes ($d = 0.1, 1.0$ and 2.0) and cuboctahedral structure.

Figure 2 presents the average magnetic moment M per atom in the ground states as a function of N with $d = 0.1, 1.0$ and 2.0, and experimental data.

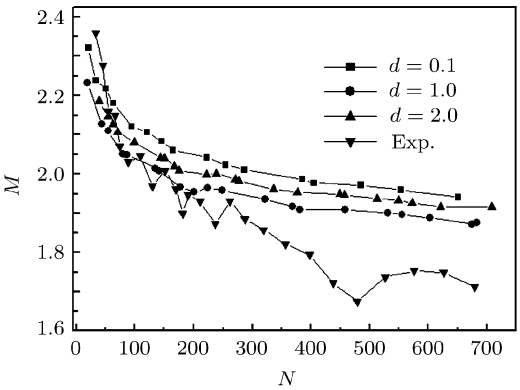


Fig.2. The average magnetic moment M per atom in the ground states as a function of N with $d = 0.1$, 1.0 and 2.0 and experimental data[16].

It is evident that the average magnetic moment decreases in an oscillatory way with the increase of clus-

ter size, which is associated with the oscillatory variation of coordination number as seen in Fig.1. In the meantime, it is found that the shape of the cluster has an important influence on the coordination number and magnetic moment, and $M(d = 0.1) > M(d = 2) > M(d = 1)$. The calculated results are similar to those for Fe cluster.[21−23] However, comparing with the experimental data, we find two obvious differences as follows: (1) the experimental oscillatory frequency and scope all exceed the simulated ones in magnitude; (2) the calculated moment for the clusters with $N > 200$ is larger than the measured one. The above two key differences indicate that the experimental results cannot be entirely explained using the geometrical structure effect (shell model). What else should be considered? Based on experimental fact that the moment is measured at a finite temperature, the moment μ_i per atom in the cluster may be excited, from which, thus it can be deduced that the thermal fluctuation effect may play an important role. It is assumed that the moments of the cluster are initially in the ground states. At a finite temperature, after running some MCS (time interval) or after thermal relaxation, the spin state of the cluster is changed from the ground state to the excited states with complex spin configurations formed. Thus, the thermal fluctuation may influence strongly the average moment of the cluster, and the vector sum of the moments in Eq.(2) should be used. Figure 3 shows N dependences of M for $d = 1$ with different MCSs at $T = 0$ K, 78 K, 160 K and 230 K, respectively.

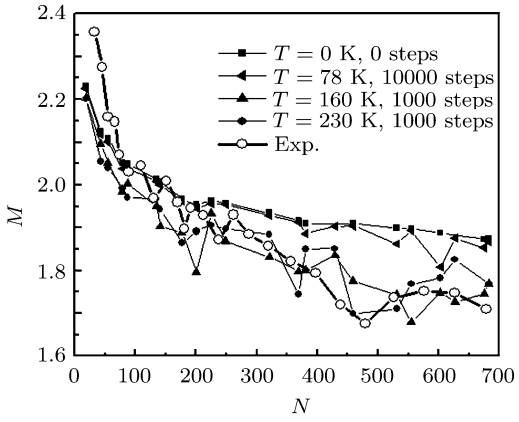


Fig.3. The moment M as a function of N with $d = 1.0$, $T = 0$ K, 78 K, 160 K and 230 K and responding to 0, 10000,1000, 1000 MC steps.

It is found that at a finite temperature, the oscillatory frequency and scope of attenuation of M increase significantly, and the moments for the clusters with $N > 200$ are close to the experimental ones, which explains the experimental results well. But then, one notes that the more consistent temperature between experiment and simulation is $T = 160$ K or 230 K, but not 78 K (measured temperature), which will be further studied. Of course, the trends of variation for the three cases are similar. Therefore, we can conclude that the oscillations superimposed on the moment decreasing moment are associated with not only the geometrical structure effects but also the thermal fluctuation.

The typical M vs T curves of the spherical PFFC with $N = 55$, 249, 2123 and the block with PB condition are shown in Fig.4. For the ferromagnetic materials, Bloch exponent law, $M(T) = M(0)(1 - BT^b)$, is often used to discuss the temperature dependence of magnetization.[31,37]

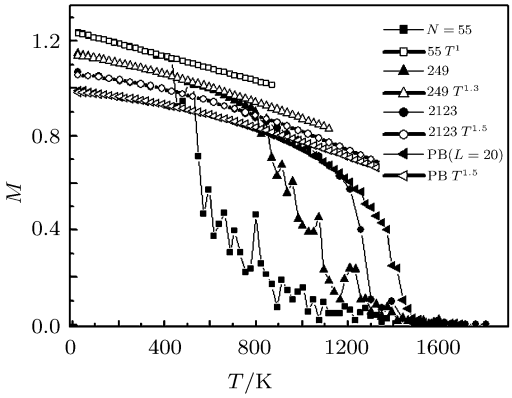


Fig.4. The typical M vs T curves of the spherical PFFC with $N = 55$, 249 and 2123 and the block with PB condition.

Here b is the Bloch exponent, and B is the Bloch constant. In order to study in detail the temperature dependence of magnetization, we fit the above M vs T curves using the Bloch exponent law. For free spherical Co clusters, in a low temperature region, M vs T curves with different N are described as follows: for $N = 55, M(T) = 1.240 \times 10^{-4}T - 2.567 \times 10^{-4}T$; for $N = 249, M(T) = 1.142 \times 10^{-5}T^{1.3} - 3.424 \times 10^{-5}T^{1.3}$; for $N = 603, M(T) = 1.099 \times 10^{-5}T^{1.4} - 1.618 \times 10^{-5}T^{1.4}$; for $N = 1061, M(T) = 1.074 \times 10^{-5}T^{1.5} - 0.794 \times 10^{-5}T^{1.5}$; for $N = 2123, M(T) = 1.056 \times 10^{-5}T^{1.5} - 0.761 \times 10^{-5}T^{1.5}$; for PB block ($L = 20$), $M(T) = 0.983 \times 10^{-5}T^{1.5} - 0.660 \times 10^{-5}T^{1.5}$. Comparing with the thermal magnetization for the Co cluster embedded in the matrices,[31] the differences between the embedded and free Co clusters are described as follows: (1) for the free cluster, the Bloch exponent b increases from 1 to 1.5 with the increase of cluster size, while for the embedded cluster the value of b remains to be 1.5 for different N. (2) For free cluster, the moment decreases with the increase

of N, which is attributed to the increase in moment due to band narrowing as a result of reduced coordination at the surface; but for the embedded cluster the moment increases with the increase of N due to an increase in Z. (3) For the above two clusters, each B increases drastically with N reducing, which is consistent with B as a function of iron crystalline size.[37] For the free Co cluster, comparing the simulation result with the experimental $M-T$ curve,[16] yields: (1) the moment decreases with N increasing; (2) when $T < 0.6T_c$, the moment is larger than that of the bulk (the block with PB condition). However, the difference between the experiment result and the simulation result still exists. For example, it is not well explained that the moment increases slightly with the increase of temperature in a low temperature region and the moment of the free cluster is smaller than that of the bulk in a high temperature region, which will be improved further.

Figure 5 (a) shows the hysteresis loops of PFFC with $N = 2123$ and $d = 1.0, T = 23, 92, 342$ and 800K. The typical hysteresis loops of the surface, the core and total clusters for PFFC with different shapes ($d = 0.1, N = 247; d = 1.0, N = 249; d = 2.0, N = 239$) at $T = 92$ K are shown in Figs.5(b), 5(c) and 5(d), respectively.

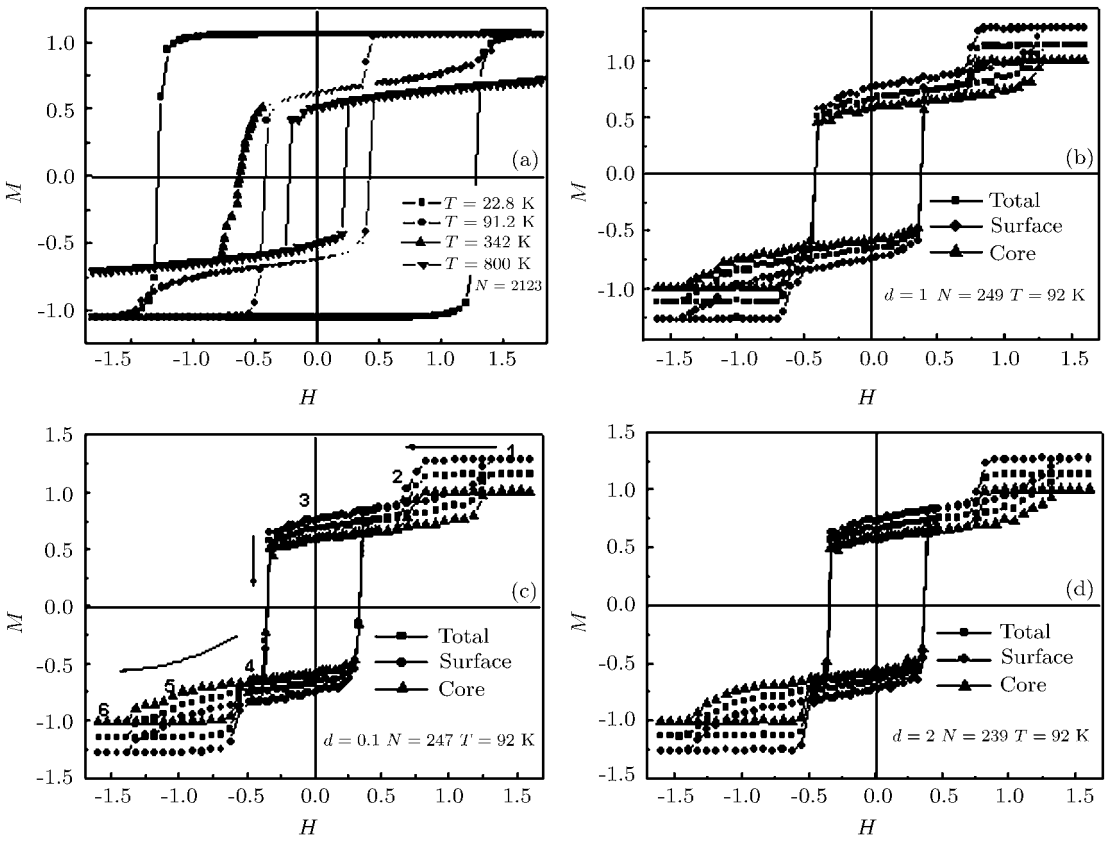


Fig.5. The hysteresis loops of PFFC with $N = 2123$, $d = 1.0$, $T = 23$, 92, 342 and 800 K(a); and the hysteresis loops of the surface, core and total clusters for the PFFC with (b) $d = 0.1$, $N = 247$, $T = 92$ K, with (c) $d = 1.0$, $N = 249$, $T = 92$ K, and with (d) $d = 2.0$, $N = 239$ and $T = 92$ K.

Figure 6 shows the spin configurations at different magnetization levels numbered in Fig. 5(c). From Figs.5–6, it is found that in a very low temperature region the loops of the cluster are perfect square; in a middle temperature region such as $T = 40 - 180$K, there exist three jumps in the loops; in a higher temperature region, there appears a progressive magnetization with single jump. In the meantime, one can also note that the saturation field and the high field susceptibility increase with cluster size decreasing or temperature increasing, which means a typical feature associated with spins disordered due to the finite-size and surface effects. From Figs.5(b)–5(d), one notes that the clusters for different shapes with nearly the same number of atoms ($N = 247$, 249 and 239) have similar loops in shape. Although magnetization in the surface is larger than that in the core due to the decreasing of coordination number in the surface, mag-

netic states in the surface and in the core jump simultaneously from one metastate to another one, which is also evidently shown in Fig.6. From the spin configurations at different magnetization levels, we can clearly find two easy axes.

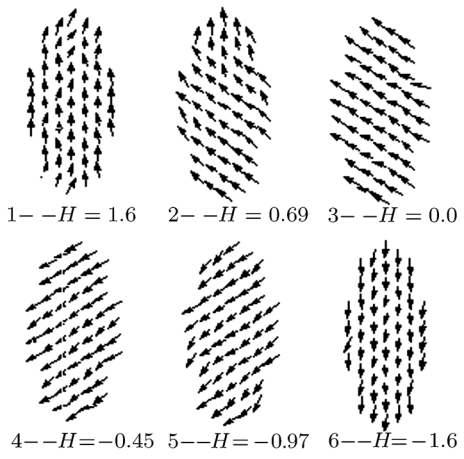


Fig.6. The spin configurations at different magnetization levels corresponding to the loops in Fig.5(c).

Figure 7(a) shows the temperature dependences of the coercivity for the ferromagnetic clusters with $K = 1$ for $N = 2123$ and 249, respectively. Figure 7(b) shows the temperature dependences of the coercivity of PFFC for $d = 1.0$ with $N = 2123$, 249, for $d = 0.1$ with $N = 247$, and for $d = 2.0$ with $N = 239$, respectively.

In the previous studies,[38,39] the temperature dependences of the coercivities for the particles are described by $H_c = H_c(0)[1 - c_a T^a]$, where $H_c(0)$ is the coercivity at $T = 0$K, c_a is the parameter related to the anisotropy, the volume of the particle and the measuring time. The exponent is a=0.5 for an assembly of aligned particles [36] and a=0.77 for randomly oriented particles.[39] The simulation results in Fig.7 indicate that, the coercivity decreases dramatically with temperature increasing in a low temperature region ($T <$ 92K) and retains almost constant in a middle temperature region, and drops again with temperature increasing in a high temperature region. The above simulated thermal coercivity is consistent with that measured in the ultra-fine iron particles,[40] nanometre-sized iron clusters,[41] γ-Fe_2O_3 nanoparticles [42,43] and $Co_{0.2}Zn_{0.8}$-Fe_2O_4 spinel oxide.[44] Therefore, for the magnetic clusters, the temperature dependence of the coercivity cannot be described by T^a law in the whole temperature region. As found in Figs.7(a) and 7(b), the magnitude of coercivity for the ferromagnetic clusters with the uniaxial anisotropy is much larger than that for PFFC, but the temperature dependence of coercivity is similar, which means that there exists a new uniaxial-like anisotropy in PFFC. Comparing with the thermal coercivity curves for different shapes ($d = 0.1, 1.0$, and 2.0) as seen in Fig.7(b), one can note that, as the cluster shape is changed from spheric ($d = 1.0$) to elongated ($d = 0.1$) or flat ($d = 2.0$) ellipse, the coercivity correspondingly decreases, which may be due to the increase in ratio of number of surface atoms to the total number of atoms. In addition, as seen from Fig.7(b), a minimum of the coercivity is found at $T = 92$ K for PFFC, which may be associated with the temperature dependence of the barrier height in the cluster and the thermal fluctuation.

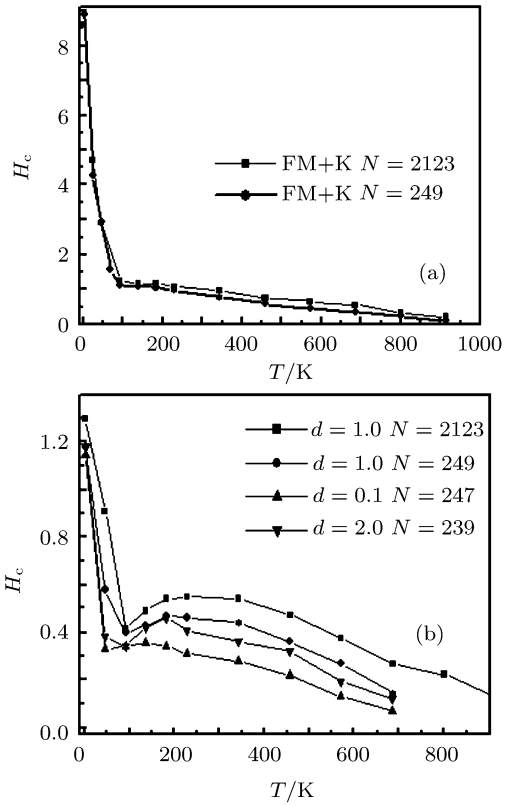


Fig.7. (a) The temperature dependences of the coercivity for the ferromagnetic clusters with $K = 1$ for $N = 2123$ and 249; (b)the temperature dependences of the coercivity of the PFFC for $d = 1.0$ with $N = 2123$ and 249, for $d =$ 0.1 with $N = 247$,and for $d = 2.0$ with $N = 239$.

The natural angle is defined as the equilibrium orientation of the ferromagnet in zero field applied, which means in fact an easy magnetization direction. It can be determined by the average orientation of the spins in zero applied fields and the spatial distribution of the energy with a probing field applied. Figures 8(a) and 8(b) show the typical spatial distributions of the energy with a probing field ($H = 0.5$) applied for PFFC with $N = 2123$ at $T = 23$ K and 92 K, respec-

tively. It is found that a multi-valley energy structure exists in a very low temperature region ($T < 40$ K).However, when $T > 40$ K, a symmetric energy distribution with two easy magnetization axes is found in Fig.8(b). From the figure, one notes that there are two energy maxima E_0 and E_{90} at θ=0°(180°), 90°(270°), respectively.

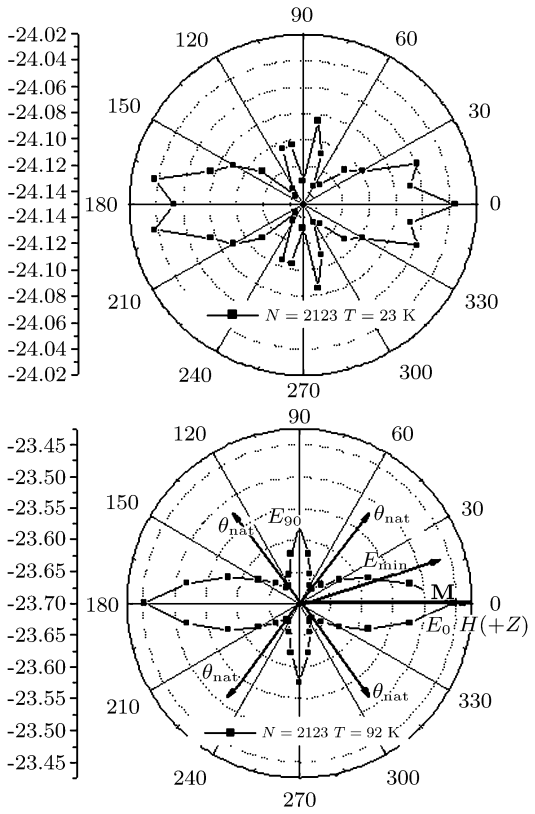


Fig.8. The typical spatial distributions of the energy with a probing field ($H = 0.5$) applied for the PFFC with $N =$ 2123 at (a)$T = 23$ K; (b)$T = 92$ K.

An energy minimum $E_{\min}$ exists between 0° and 90°. The natural angle for PFFC with $N = 2123$ at $T = 92$ K is also shown in Fig.8(b). It can be found that the orientation of the energy minimum of the cluster derived from the direction of the natural angle is consistent with that from the energy distribution. The barrier heights $(E_0 - E_{\min})$ and $(E_{90} - E_{\min})$ as a function of temperature for PFFC with $N = 2123$ are shown in Fig.9. From the figure, it is found that in a low temperature region ($T < 100$ K), the barrier heights of the cluster decrease dramatically with temperature decreasing; in a middle temperature region (100 K $< T <$ 700 K), they increase slightly with temperature increasing; in a high temperature region ($T >$ 700K), they increase evidently with the increase of temperature. Figure 10 shows the natural angle as a function of temperature for PFFC with $N = 2123$. From the figure, it is found that, as the temperature increases slightly, the natural angle jumps sharply to ∼50°. Then when 20 K $< T <$ 900 K, it remains about at $\theta_{\rm nat}$≈50°.

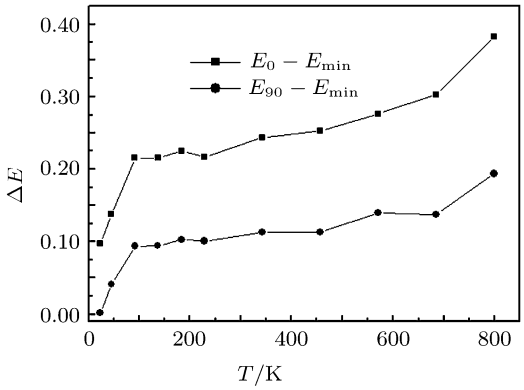


Fig.9. The barrier heights $(E_0 - E_{\min})$ and $(E_{90} - E_{\min})$ with $N = 2123$ as a function of temperature for PFFC.

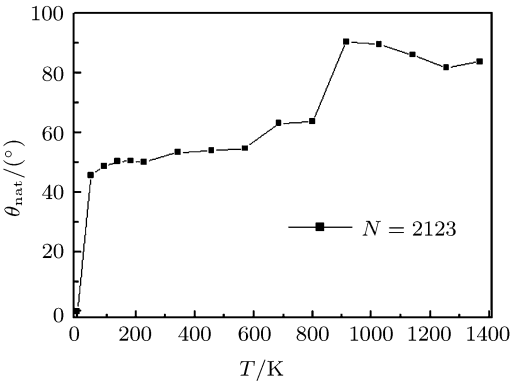


Fig.10. The natural angle as a function of temperature for PFFC with $N = 2123$.

Moreover, when $T >$ 900 K, the natural angle jumps to ∼90°, which is due to the enhancement of disorder degree of the spins. We also obtain the typical spatial distributions of the energies with a probing field ($H = 0.5$) applied for PFFC at $T = 92$ K with $d = 0.1$ and $N = 247$; $d = 1.0$ and $N = 249$; $d = 2.0$ and $N = 239$, respectively. It is found that although the energies for $d = 0.1$ and 2.0 are both larger than the energy for $d = 1.0$ due to the decrease in average coordination number, three free ferromagnetic clusters with zero anisotropy have similar energy distributions. The natural angle and energy distributions as seen in Figs.8–10 indicate clearly the existence of the configurational anisotropy for the free ferromagnetic clusters with zero anisotropy, which are consistent with those in the elliptical, triangular, square, pentagonal and circular geometries.[25−27] The simulated results are also similar to those for the embedded magnetic clusters.[36]

Now we use the natural angle and configurational anisotropy to discuss the magnetization behaviour of

the clusters as seen in Figs.5–7. In a low temperature region ($T < 40$ K), the multi-valley energy structure as seen in Fig.8(a) gives rise to a local energy minimum at $\theta = 0°$, and a small thermal energy $k_{\rm B}T$. Therefore the magnitude of the magnetization remains at a saturated value until the reversal point where the magnetization jumps to another metastable state is reached. The jump occurs when the Zeeman energy exceeds the barrier from the anisotropy energy. Thus, the loop is square in shape at very low temperatures, as seen in Fig.5(a). In a middle temperature region (46 K $< T <$ 184 K), the loop shapes and the spin configurations of the cluster in the magnetization process as found in Fig.5 can be explained as follows: the magnetization states of the cluster are mainly determined by the configurational anisotropy energy $E_{\rm K}$, Zeeman energy $E_{\rm h}$ and thermal energy $k_{\rm B}T$. When the applied field is large enough to overcome the thermal fluctuation, the spins are forced to be along the direction of the applied field (Z-axis) and remain to be at the saturation state. When the applied field decreases and the thermal energy is above the Zeeman energy, the spins wriggle themselves freely to jump to the easy magnetization direction as seen in the states '2' and '3' in Figs.5–6, and Fig.8(b). When the Zeeman energy changes from '–' to '+', the thermal and Zeeman energies both overcome the barrier to reverse the spins. When the applied field equals the coercivity, the spins jump to another easy magnetization direction as found in the state '4'. When the applied field increases gradually along the negative Z-axis direction, the spins are forced to rotate to the negative Z-axis direction. In a higher temperature region ($T >$ 184K), the thermal energy is higher than the Zeeman energy, which leads the spins to be initially in the easy magnetization direction. Therefore only one coherent jump exists as seen in Fig.5(a). The barrier height of the cluster decreases with temperature decreasing as seen in Fig.9, which gives rise to a decrease in coercivity. In contrast, the decrease in temperature causes the coercivity to increase due to the decreasing of thermal fluctuation. In addition, the natural angle (easy magnetization direction) remains almost constant in a middle temperature region (20 K $<$ T $<$ 900 K) as seen in Fig.10. Therefore, the three factors above determine together the thermal dependences of the coercivity, especially, the appearance of minimum at $T \simeq$92 K as seen in Fig.7(b).

4. Conclusions

The average magnetic moments as a function of the cluster size with different shapes are presented for free Co cluster. It is thought that the oscillations superimposed on the decreasing moment are attributed to not only the geometrical structure effects but also the temperature effects. Comparing the thermal magnetization of the free Co cluster with that of Co cluster embedded in the matrices, their difference is found. The simulated thermal dependence of the coercivity reveals that the coercivity decreases dramatically with the increase of temperature in a low temperature region ($T <$ 100 K), retains almost constant at the middle temperature region, and decreases again with temperature increasing in a high temperature region. This temperature dependence of the coercivity is consistent with the experimental result, but does not fit the T^a law in the whole temperature region. The hystereses and thermal coercivities for free clusters with zero and finite uniaxial anisotropies are calculated. It is evident that an easy magnetization direction and an anisotropy resulting from the spin configurations exist in the free clusters with the pure exchange interaction. The simulation results for the nature angle and energy distribution in the clusters prove further the existence of the configurational anisotropy. By introducing the natural angle and configurational anisotropy, the relationship between natural angle and coercivity is discussed.

References

[1] Allenspach R and Bishchof A 1992 *Phys. Rev. Lett.* **69** 3385

[2] Freeman A J and Wu R Q 1991 *J. Magn. Magn. Mater.* **100** 497

[3] Fert A, Grunberg P, Barthelemy A, Petroff P and Zinn W 1995 *J. Magn. Magn. Mater.* **140-144** 1

[4] Parkin S S S 1991 *Phys. Rev. Lett.* **67** 3598

[5] Shi Jing, Gider S, Babcock K and Awschalom D D 1996 *Science* **271** 937

[6] Chien C L 1995 *Annu. Rev. Mat. Sci.* **25** 129

[7] Moodera J S, Kinder L R, Wong T M and Meservey R 1995 *Phys. Rev. Lett.* **74** 3273

[8] Chen P, Xing D Y, Du Y W, Zhu J M and Feng D 2001 *Phys. Rev. Lett.* **87** 107202-1

[9] Versluijs J J, Bari M A and Coey J M D 2001 *Phys. Rev. Lett.* **87** 026601
[10] Holdenried M, Hackenbroich B and Micklitz H 2001 *J. Magn. Magn. Mater.* **231** L13
[11] Zhang N, Ding W P, Zhong W, Xing D Y and Du Y W 1997 *Phys. Rev.* B **56** 8138
[12] Huang Z G, Chen Z G, Peng K, Wang D H, Zhang F M, Zhang W Y and Du Y W 2004 *Phys. Rev.* B **69** 094420
[13] Ziese M 1999 *Phys. Rev.* B **60** R738
[14] Coex D M, Trevor D J, Whetten R L, Rohlfing E A and Kaldor A 1985 *Phys. Rev.* B **32** 7290
[15] De Heer W A, Milani P and Chatelain A 1990 *Phys. Rev. Lett.* **65** 488
[16] Billas I M L, Chatelain A and de Heer W A 1994 *Science* **265** 1682; 1997 *J. Magn. Magn. Mater.* **168** 64
[17] Liu F, Khanna S N and Jena P 1990 *Phys. Rev.* B **42** 976
[18] Pastor G M, Dorantes-Davila J and Bennemann K H 1989 *Phys. Rev.* B **40** 7642
[19] Tischer M, Hjortstam O, Arvanitis D, Dunn H J, May F, Baberschke K, Trygg J, Wills J M, Johansson B and Eriksson O 1995 *Phys. Rev. Lett.* **75** 1602.
[20] Rosengaard N M and Johansson B 1997 *Phys. Rev.* B **55** 14975
[21] Zhao J, Chen X, Sun Q, Liu F and Wang G 1995 *Phys. Lett.* A **205** 308
[22] Jensen P J and Bennemann K H 1995 *Z. Phys.* D **35** 273
[23] Aguilera F, Montejano-Carrizales J M and Moran-Lopeze J L 1998 *Phys. Lett.* A **242** 255
[24] Stoner E C and Wohlfarth E P 1991 *IEEE Trans. Magn.* **27** 3475
[25] Cowburn R P 2000 *J. Phys.* D: *Appl. Phys.* **33** R1
[26] Cowburn R P, Koltssov D K, Adeyeye A O and Welland M E 1999 *Europhys. Lett.* **48** 221
[27] Cowburn R P, Adeyeye A O and Welland M E 1998 *Phys. Rev. Lett.* **81** 5414
[28] Torres L, Martinez E, Lopez-Diaz L and Iniguez J 2001 *J. Appl. Phys.* **89** 7585
[29] Stamp R L 2000 *J. Phys.* D: *Appl. Phys.* **33** R247
[30] Kim J V , Stamps R L, McGrath B V and Camley R E 2000 *Phys. Rev.* B **61** 8888
[31] Huang Z G and Du Y W 2002 *Phys. Lett.* A **300** 641
[32] Vargas P, Altbir D and d'Albuquerque Castro J 2001 *J. Magn. Magn. Mater.* **226-230** 603
[33] Binder K and W Heermann D 1992 *Monte Carlo Simulation in Statistical Physics* (Berlin: Springer)
[34] Feng Q, Huang Z G and Du Y W 2003 *Acta Phys. Sin.* **52** 2906
[35] Weng Z Z, Feng Q, Xiao Y, Huang Z G and Du Y W 2004 *Acta Phys. Sin.* **53** 3177
[36] Huang Z G, Chen Z G, Zhang F M and Du Y W 2004 *Eur. Phys. J.* B **37** 177
[37] Zhang D J, Klabunde K J, Sorensen C M and Hadjipanayis G C 1998 *Phys. Rev.* B **58** 14167
[38] Bean C P and Livingston J D 1959 *J. Appl. Phys.* **30** 120S
[39] Pfeiffer H and Schuppel W 1990 *Phys. Status Solidi* A **119** 259.
[40] Jen S U, Lee C Y and Yao Y D 1991 *J. Magn. Magn. Mater.* **96** 82
[41] Johansson C, Aklint T, Hanson M, Andersson M, Tarras-Wahlberg N, Olsson E, Kalska B, Wappling R and Rosen A 1999 *Nanostructured Materials* **12** 287
[42] Martinez B, Obradors X, Balcells L I , Rouanet A and Monty C 1998 *Phys. Rev. Lett.* **80** 181.
[43] Martinez B, Roig A, Obradors X and Molins E 1996 *J. Appl. Phys.* **79** 2580
[44] Bhowmik B N and Ranganathan R 2002 *J. Magn. Magn. Mater.* **248** 101